

Light-Sensitive Ruthenium Complex-Loaded Cross-linked Polymeric Nanoassemblies for the Treatment of Cancer

Matthew Dickerson, Brock Howerton, Younsoo Bae, and Edith Glazer

Supporting Information

1. Verification of PEG-BLA block copolymer synthesis using $^1\text{H-NMR}$
2. Monitoring of the photoactivation of 1 and 2 using HPLC
3. The effect of solution ionic strength on the spectral properties of the prodrug and photoactivated forms of 1 and 2
4. GPC trace of 3-loaded PEG-ASP CNAs compared to empty PEG-ASP CNAs
5. DNA precipitation induced by 2 and 3 on agarose gels in the dark
6. Light-activated IC_{50} curves for free Ru complexes and Ru complex-loaded PEG-ASP CNAs in A549 cells
7. Washout study (8 hrs) IC_{50} curves for light-activated free Ru complexes and Ru complex-loaded PEG-ASP CNAs in A549 cells
8. Complex 2 characterization data
9. Complex 3 characterization data
10. Cytotoxicity studies

1. Verification of PEG-BLA block copolymer synthesis using $^1\text{H-NMR}$

After the synthesis and purification of PEG-BLA block copolymers, successful formation of the BLA block was confirmed using a 500 MHz NMR. The block copolymer was analyzed in DMSO- d_6 . The peak associated with the ester-protecting group of the BLA block was located at 7.31 ppm. The length of the BLA block was estimated based on the ratio of the benzyl ester peak to the 5,000 MW PEG peak located at 3.47 ppm (~35 units).

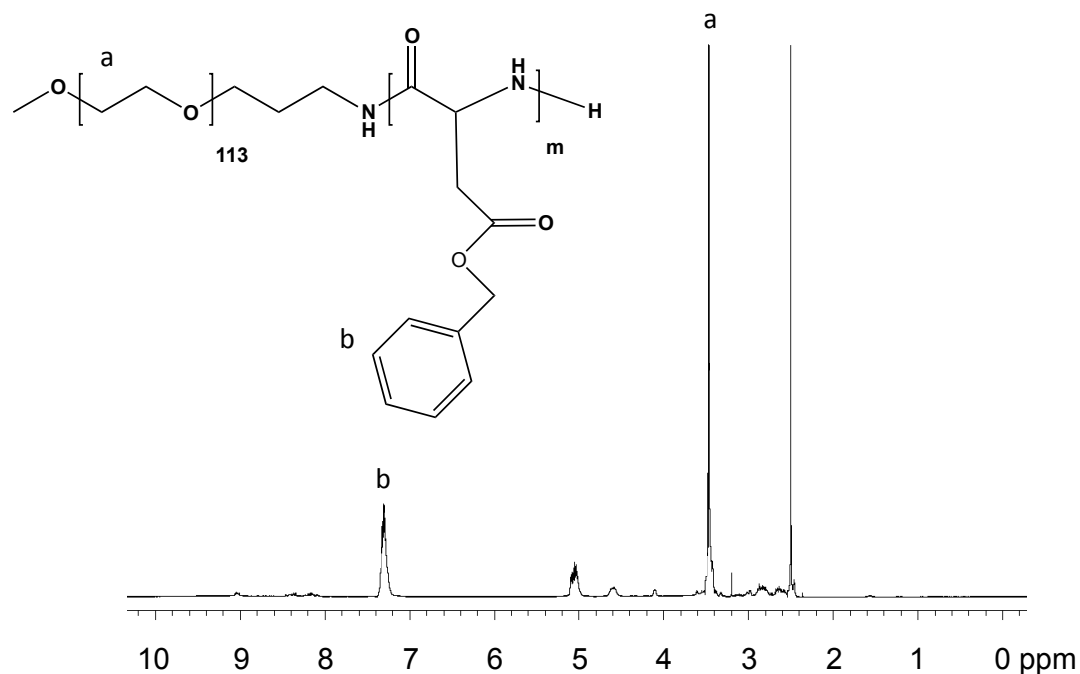


Figure S1: $^1\text{H-NMR}$ of PEG-BLA block copolymer in DMSO-d_6 .

2. Monitoring of the photoactivation of **1** and **2** using HPLC

1 and **2** were prepared at a concentration of $20\ \mu\text{M}$ ($500\ \mu\text{L}$) in diH_2O . Dmbpy was prepared at a concentration of $5\ \text{mM}$ in acetonitrile ($500\ \mu\text{L}$) for comparison. Sample absorbance was monitored at $280\ \text{nm}$ using an Agilent 1100 Series HPLC equipped with a Grace Vydac 218TP C18 column at a constant flow rate of $1\ \text{mL}/\text{min}$ ($20\ \mu\text{L}$ sample injection for **1** and **2** and $10\ \mu\text{L}$ for dmbpy) with the following gradient of diH_2O (0.1% formic acid) and MeCN (0.1% formic acid):

Time (min)	MeCN (%)	diH_2O (%)
0	2	98
2	5	95
5	30	70
20	60	40
30	95	5
35	2	98

The Ru complex samples were subsequently exposed to light ($200\ \text{W}$, $\lambda > 400\ \text{nm}$) for $10\ \text{min}$ ($7\ \text{J}/\text{cm}^2$) to induce photoejection of bidentate dmbpy ligands and analyzed again

using the same protocol detailed above. When protected from light, **1** eluted at 8.2 min and **2** eluted at 19.8 min. Dmbpy eluted at 8.2 min. After photoactivation of **1**, two peaks displaying characteristic Ru complex MLCT peaks emerged at 4.6 and 7.5 min while a peak consistent with the elution time and absorbance profile of dmbpy emerged at 8.3 min. Photoactivation of **2** led to the emergence of a peak at 16.7 min with Ru complex character and the elution of a peak consistent with dmbpy at 8.3 min. A diH₂O blank was also analyzed by HPLC as a baseline and subtracted from **1** and **2** samples (Figure S2 and S3). The impurity that eluted around 21 min was present in all samples, including the diH₂O blank (Figure S4). This indicates that it was not a result of impurities remaining in either of the Ru complex samples. The purity of **1** and **2** was determined based on peak area of samples protected from light using GraphPad Prism 5.0a. The purity of both **1** and **2** were determined to be 99%.

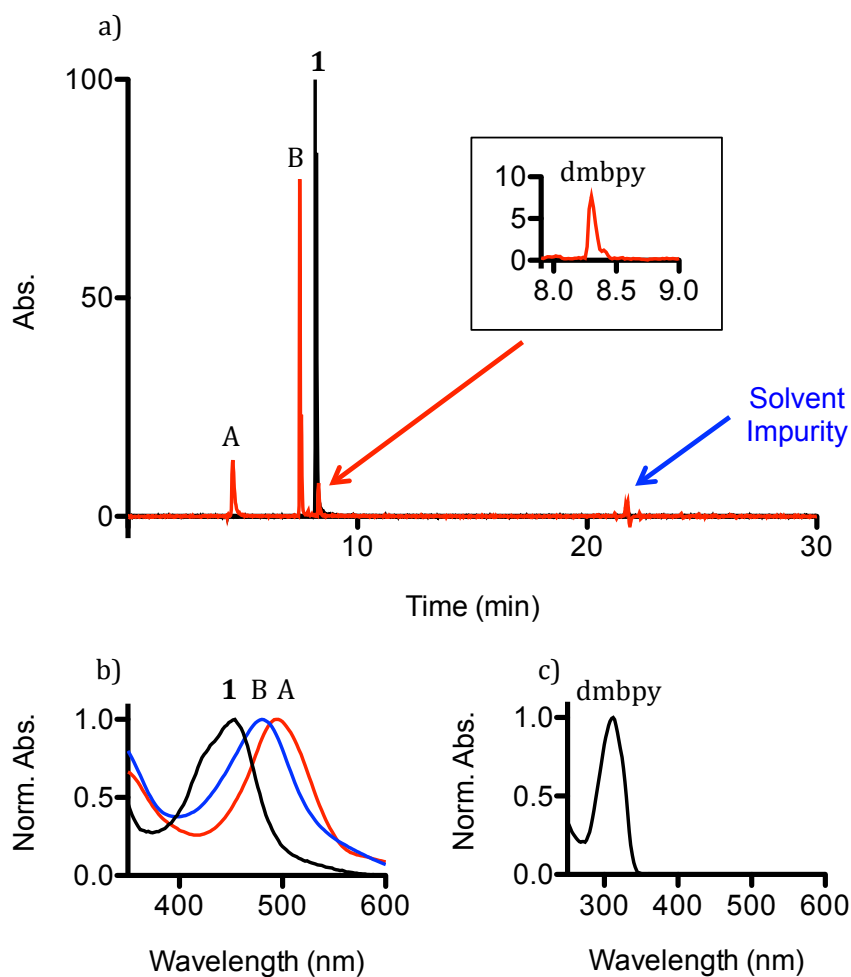


Figure S2: HPLC analysis of the photoactivation of **1**. a) Chromatograms of the prodrug (**1**; black) and the photoproducts (A, B, and dmbpy; red) of **1**. b) The corresponding spectra for **1** (black), photoproduct A (red), and photoproduct B (blue). c) The spectrum of photoejected dmbpy.

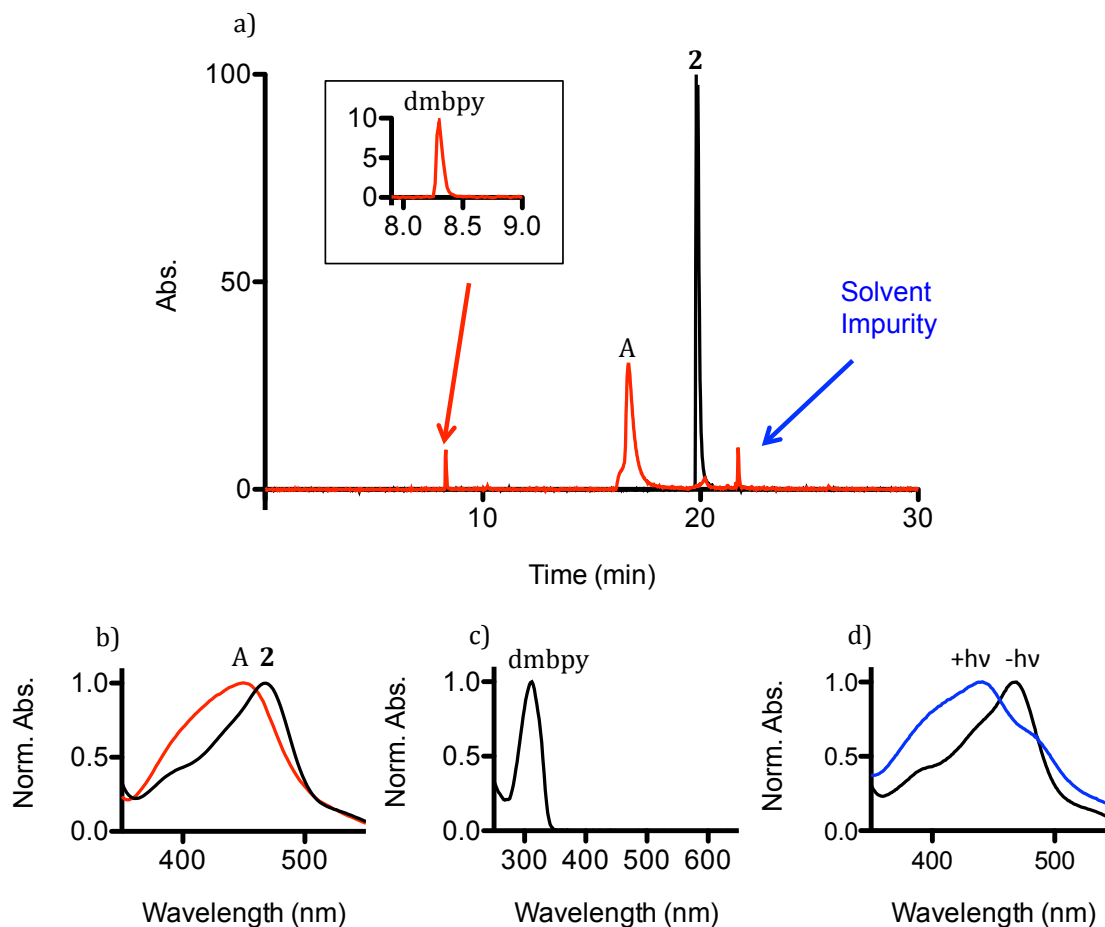


Figure S3: HPLC analysis of the photoactivation of **2**. a) Chromatograms of the prodrug (**2**; black) and the photoproduct (A, and dmbpy; red) of **2**. b) The corresponding spectra for **2** (black) and photoproduct A (red). c) The spectrum of photoejected dmbpy. d) Spectra of **2** when protected from light ($-h\nu$, black) and after 30 min irradiation (20 J/cm^2) ($+h\nu$, blue) in acetonitrile, illustrating the blue-shift initiated by photoactivation in acetonitrile compared to the red-shift observed in diH_2O and PBS (Figure 4c-d).

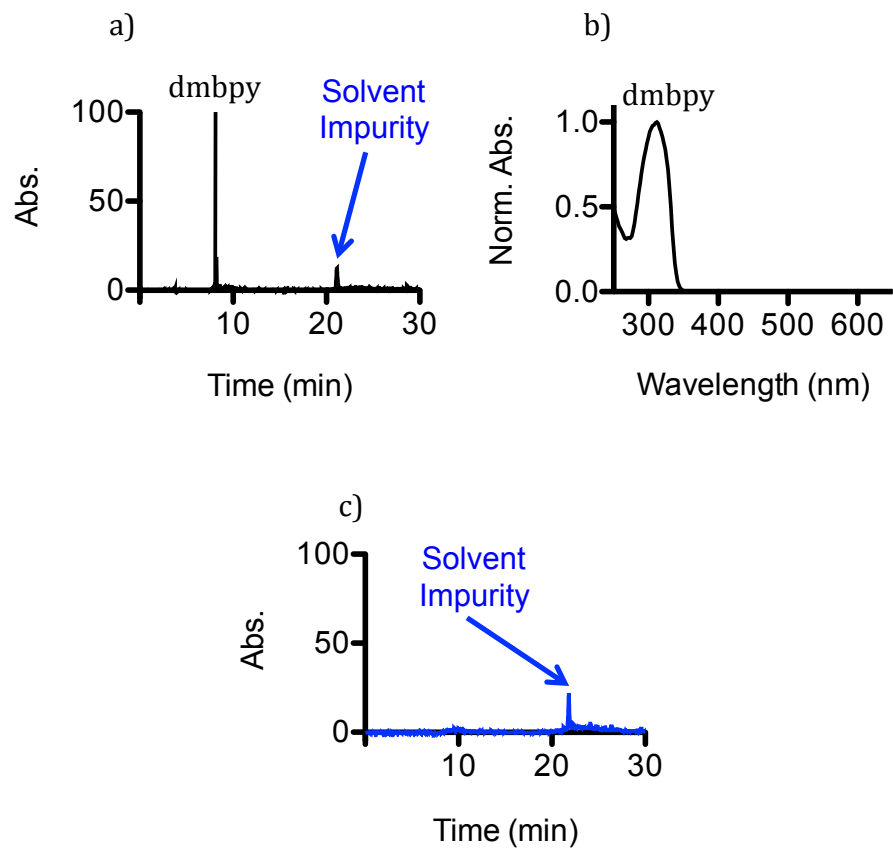


Figure S4: HPLC analysis of free dmbpy and a diH₂O blank. a) The chromatogram for free dmbpy (black). b) The corresponding absorbance spectrum of free dmbpy (black). c) The chromatogram of a diH₂O blank illustrating the observed solvent impurity.

3. The effect of solution ionic strength on the spectra of the prodrug and photoactivated forms of **1** and **2**

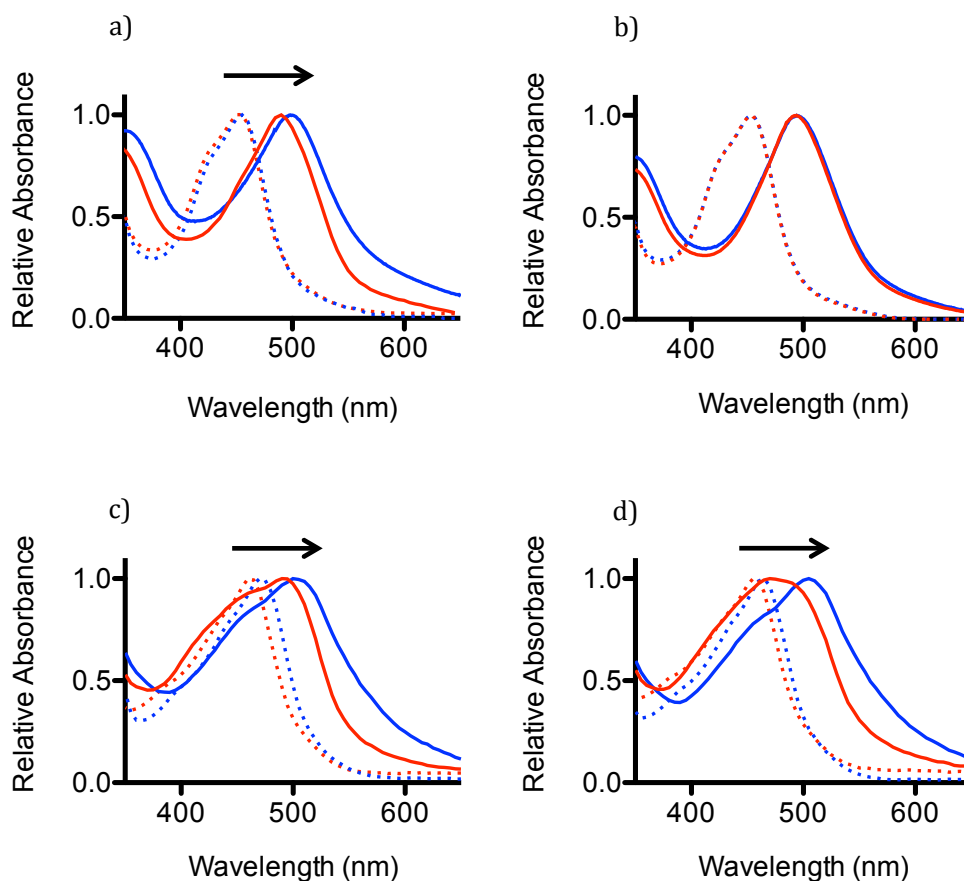


Figure S5: The effect of ionic strength on the interactions between Ru complexes and PEG-ASP CNAs for a) **1** in diH₂O and b) 100 mM NaCl and c) **2** in diH₂O and d) 100 mM NaCl (dark free complex (- - -), dark PEG-ASP CNAs (- - -), light free complex (—), and light PEG-ASP CNAs (—)). In the dark, salt concentration did not have any effect. After irradiation, a red-shift was observed for **1**- and **2**-loaded PEG-ASP CNAs in diH₂O compared to free complexes. The addition of 100 μ M NaCl led to a blue-shift in the spectra of **1**-loaded PEG-ASP CNAs to match the spectra of free **1** but did not affect the spectra of **2**-loaded PEG-ASP CNAs (black arrows indicate red shifts of Ru complex-loaded PEG-ASP CNAs compared to free Ru complexes).

4. GPC trace of **3**-loaded PEG-ASP CNAs compared to empty PEG-ASP CNAs

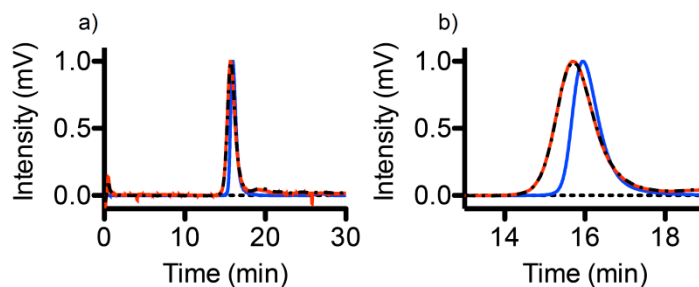


Figure S6: GPC traces of the elution of **3**-loaded PEG-ASP CNAs at 280 nm (---) and at 450 nm (—) and empty PEG-ASP CNAs at 280 nm (—). a) Shows the full 30 min time course of the experiment for both formulations while b) shows an expansion of the time interval where elution occurs. The trace for empty PEG-ASP CNAs was collected at 280 nm as indicated in the manuscript while the trace for **3**-loaded PEG-ASP CNAs was collected at 280 nm and at the MLCT peak for **3** (450 nm) where empty PEG-ASP CNAs do not display absorbance. This demonstrates that **3**-loaded PEG-ASP CNAs are similar in size to empty PEG-ASP CNAs as was observed for **1**- and **2**-loaded PEG-ASP CNAs.

5. DNA precipitation on agarose gels induced by **2** and **3** in the dark

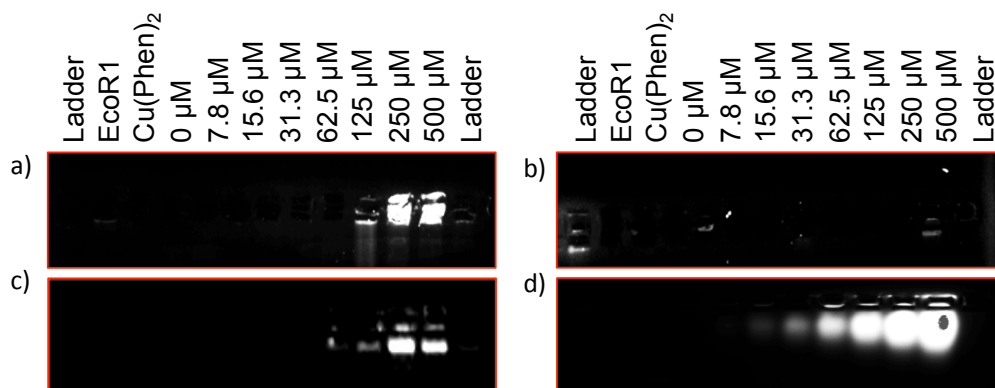


Figure S7: DNA precipitation in wells of agarose gels. a) Free **2** led to precipitation of DNA at concentrations above 125 μM while b) **2**-loaded PEG-ASP CNAs did not. c) Free **3** led to DNA precipitation at concentrations above 125 μM while d) **3**-loaded PEG-ASP CNAs did not. The **3**-loaded PEG-ASP CNAs remained nearly immobile (located just below the wells) due to their inability to migrate effectively through the agarose gel. This accounts for the luminescent response in d). As shown in Figure 8, DNA migration was unaffected by **3**-loaded PEG-ASP CNAs.

6. Light-activated EC₅₀ curves for free Ru complexes and Ru complex-loaded PEG-ASP CNAs after a 72 hr exposure time in A549 cells

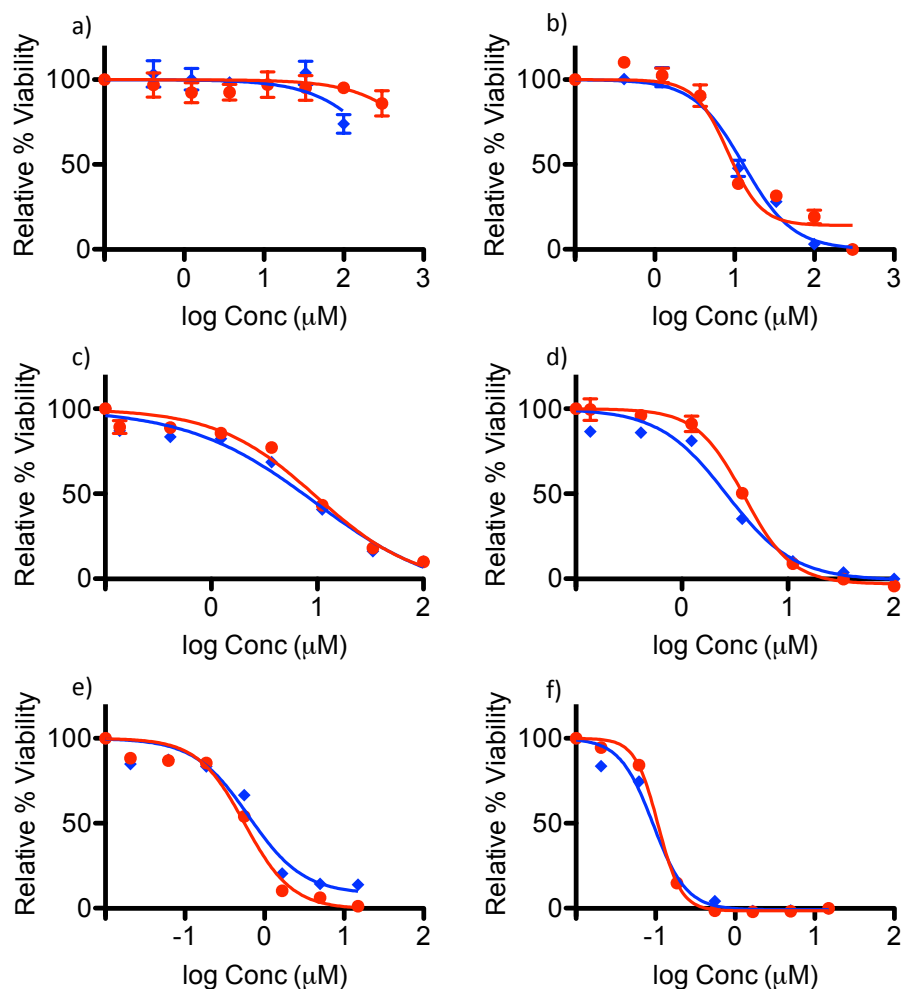


Figure S8: *In vitro* A549 EC₅₀ cell cytotoxicity (72 hrs) for a) **1** formulations protected from light and b) light-activated (irradiated with light ($\lambda > 400$ nm) in 30 sec pulses with 30 sec between pulses for a total exposure time for 5 mins), for c) **2** formulations protected from light and d) light-activated, and for e) **3** formulations protected from light and f) light-activated (free Ru complex ($\color{blue}\blacklozenge$) and Ru complex-loaded CNAs ($\color{red}\bullet$))(N = 3).

7. Washout study (8 hrs) EC₅₀ curves for light-activated free Ru complexes and Ru complex-loaded PEG-ASP CNAs in A549 cells

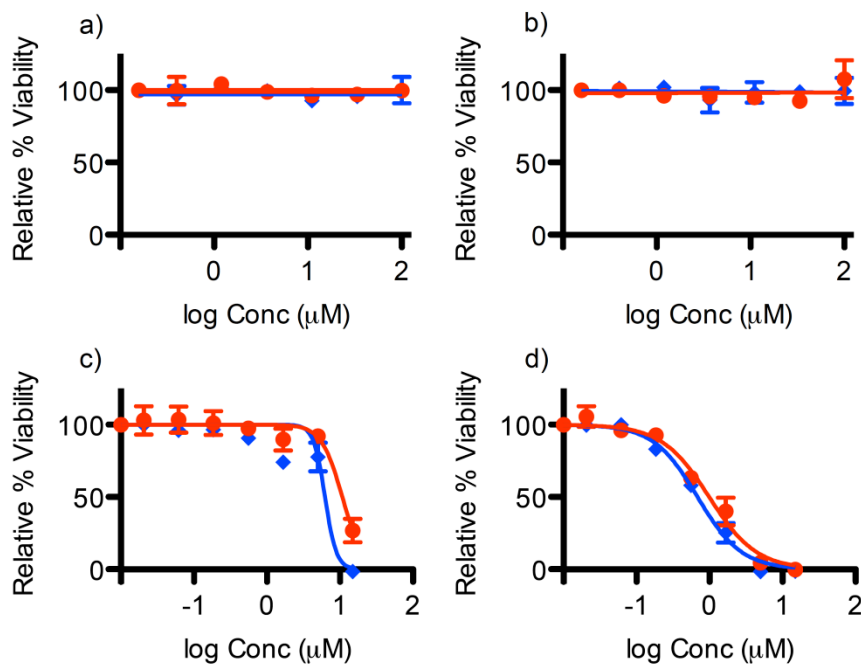


Figure S9: *In vitro* A549 EC₅₀ cell cytotoxicity following Ru complex washout. Cells were incubated with selected free and CNA entrapped Ru complexes for 8 hrs protected from light. The media containing free Ru complexes or Ru complex-loaded CNAs was aspirated off, cells were washed three times with fresh media to remove any extracellular free or CNA entrapped Ru complexes, irradiated with light ($\lambda > 400$ nm) in 30 sec pulses with 30 sec between pulses for a total exposure time of 5 min, incubated for 72 hrs at 37 °C, 5% CO₂, and viability determined using methods outlined in the main manuscript. Cytotoxicity profiles are shown for a) **1** formulations protected from light and b) light-activated, for c) complex **3** formulations protected from light and d) light-activated (free Ru complex ($\color{blue}\blacklozenge$) and Ru complex-loaded CNAs ($\color{red}\bullet$))(N = 3).

8. Complex 2 Characterization data

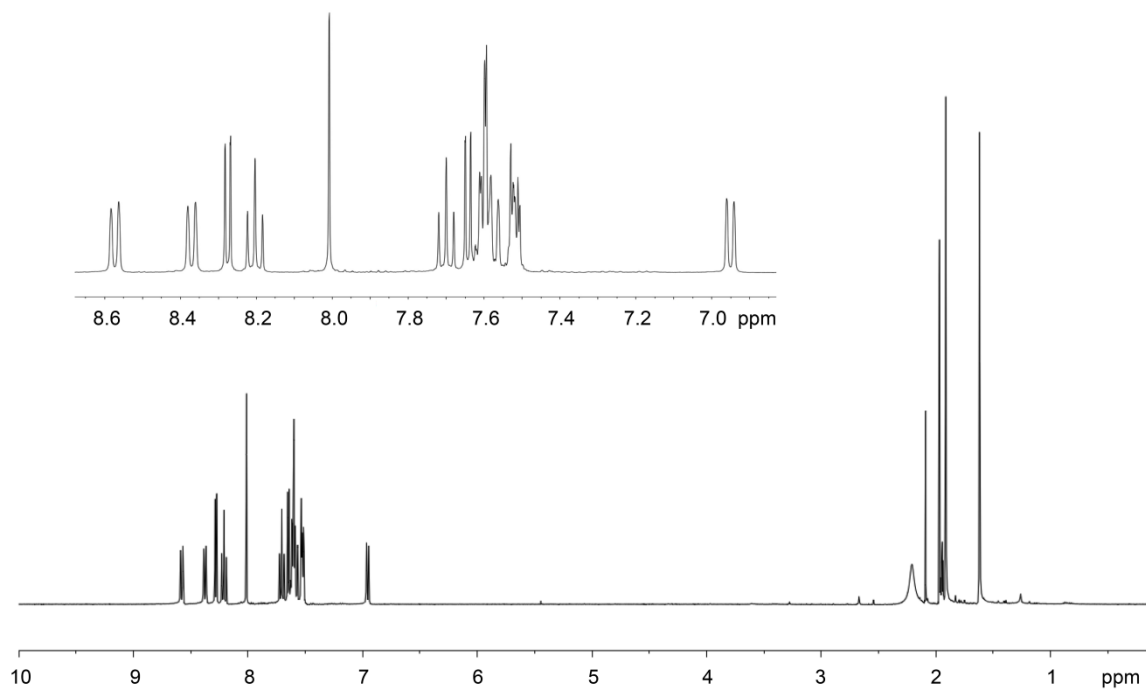
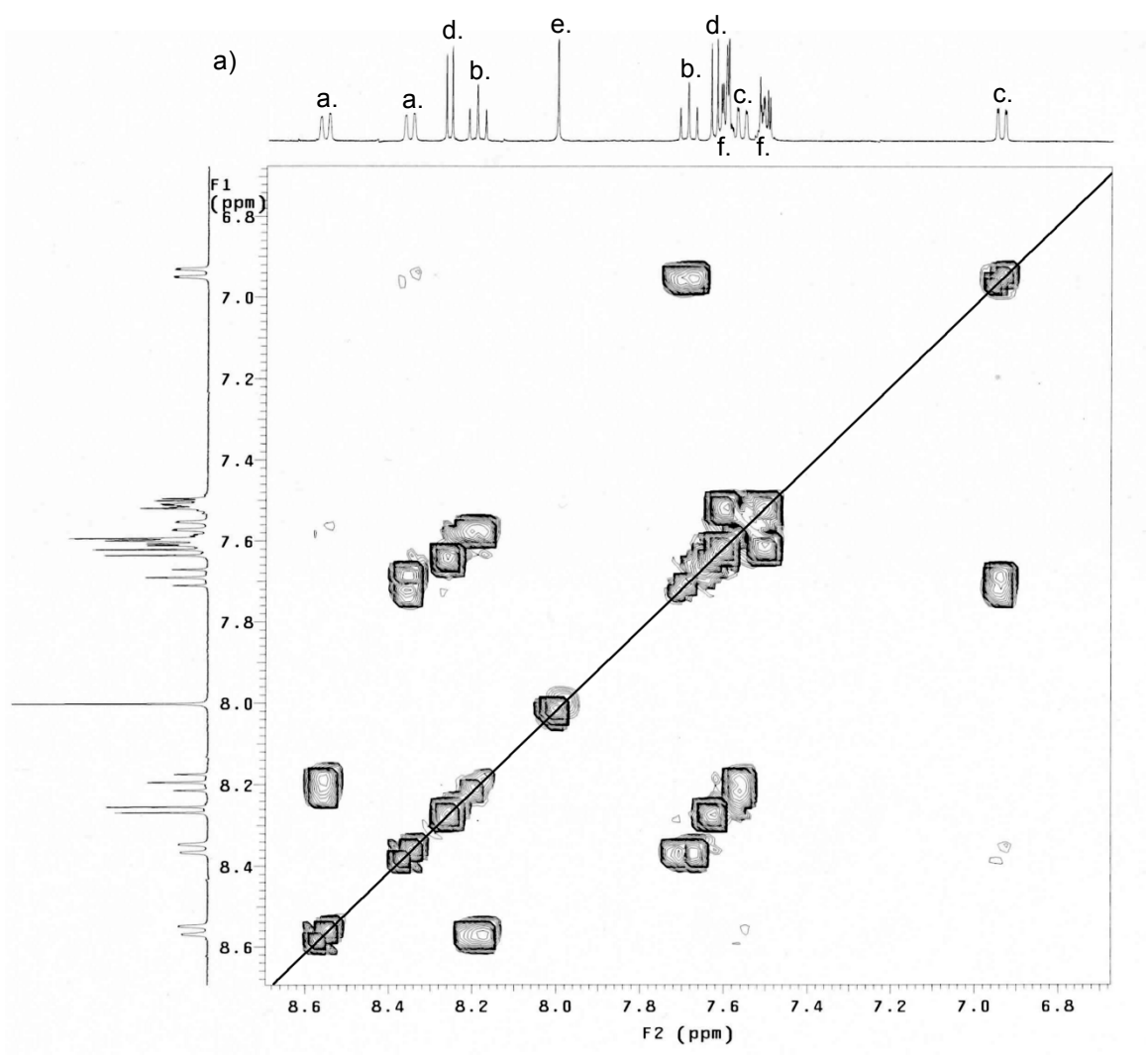
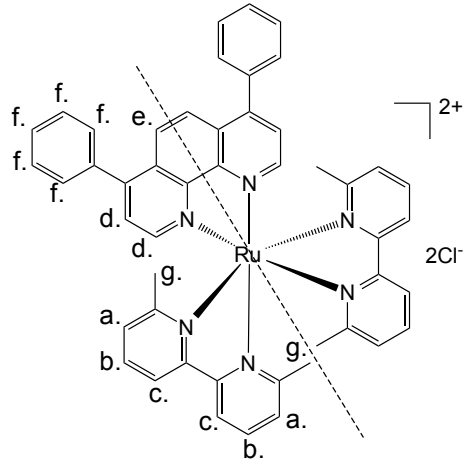


Figure S10: $^1\text{H-NMR}$ of **2** in CD_3CN . The peaks at 1.91 and 1.61 ppm are the methyl groups from dmbpy. As expected from the symmetry of the complex, 12 unique aromatic resonances were observed (some of which are overlapping).



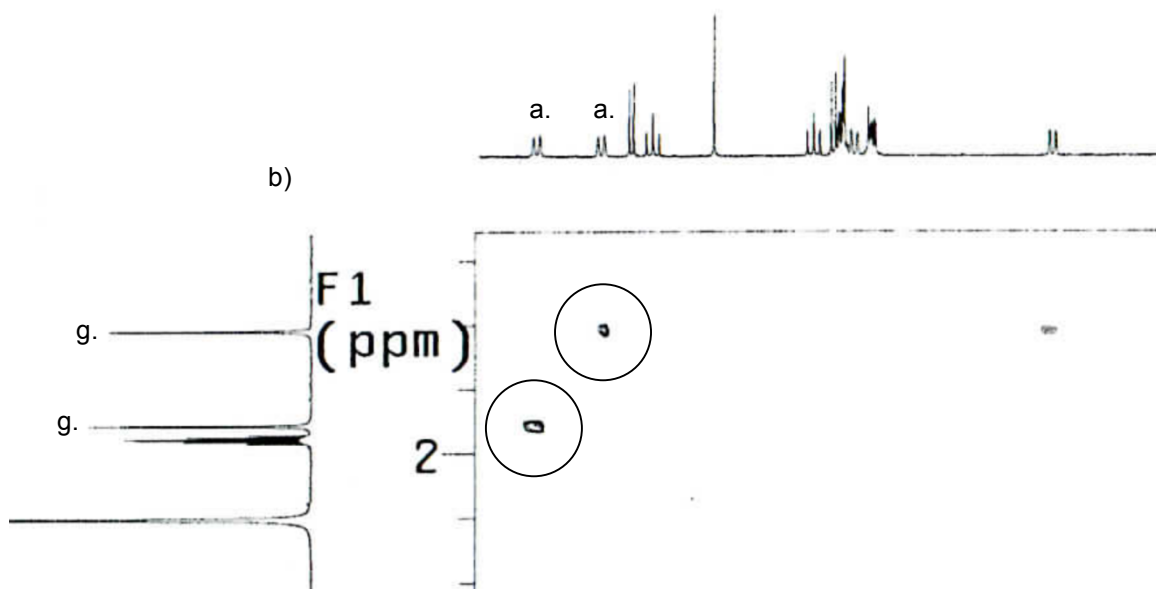


Figure S11: a) Expansion of the aromatic region of the COSY ^1H -NMR of **2** in CD_3CN . Multiple occurrences of letters denote protons that could not be precisely assigned. It does not indicate equivalency. b) Illustration of weak interactions between distant dmbpy protons and methyl groups (indicated by black circles).

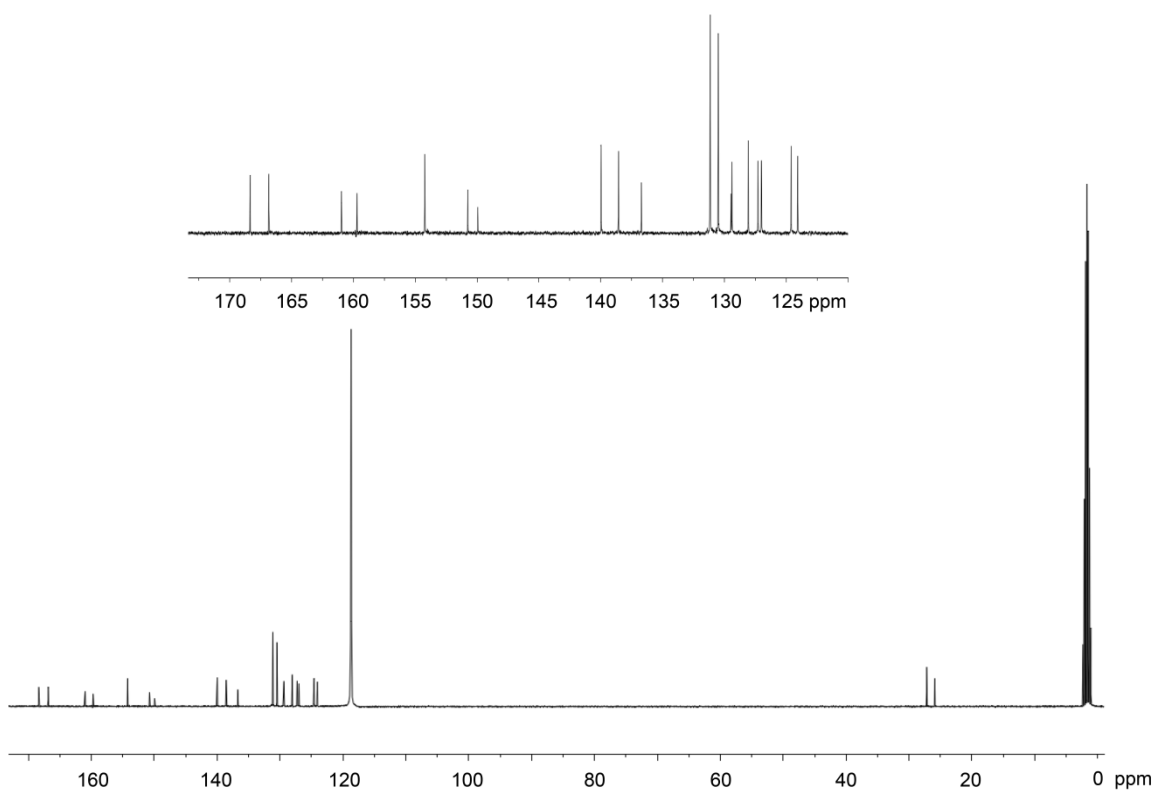


Figure S12: ^{13}C -NMR of **2** in CD_3CN . The peaks at 26.73 and 25.44 ppm are the methyl groups from dmbpy. As expected from the symmetry of the complex, 20 unique carbons were observed.

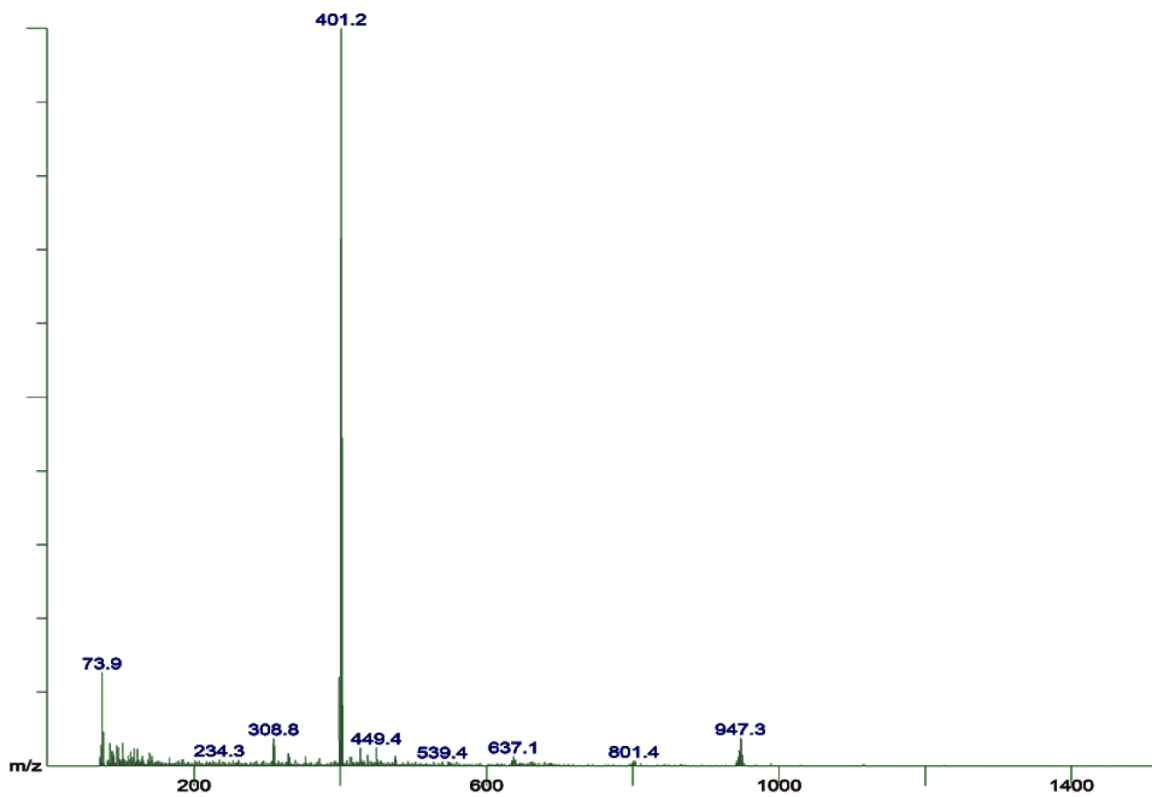


Figure S13: ESI-MS infusion of **2**. The ion at m/z 947.3 is the +1 form of the complex and the ion at m/z 401.2 is the +2 form of the complex.

9. Complex 3 characterization data

$^1\text{H-NMR}$ (CD_3CN , 400 MHz) δ : 8.29 (d, $J=5.5$ Hz, 2H), 8.23 (s, 2H), 7.66 (m, 4H), 7.62 (m, 10H). $^{13}\text{C-NMR}$ (CD_3CN , 400 MHz) δ : 154.03, 150.76, 150.21, 137.36, 131.44, 131.30, 130.77, 130.65, 127.70, 127.67. ESI MS calculated for $\text{C}_{72}\text{H}_{48}\text{N}_6\text{Ru} [\text{M}]^{2+}$ 549.1; found 549.0 $[\text{M}]^{2+}$. A peak associated with free dip was also observed at 333.0 but was not apparent in $^1\text{H-}$ and $^{13}\text{C-NMR}$ analysis. UV/Vis (diH_2O): λ_{max} nm ($\epsilon \text{ M}^{-1} \text{ cm}^{-1}$): 276 (75,400), 309 (sh), 439 (30,300), 460 (29,500).

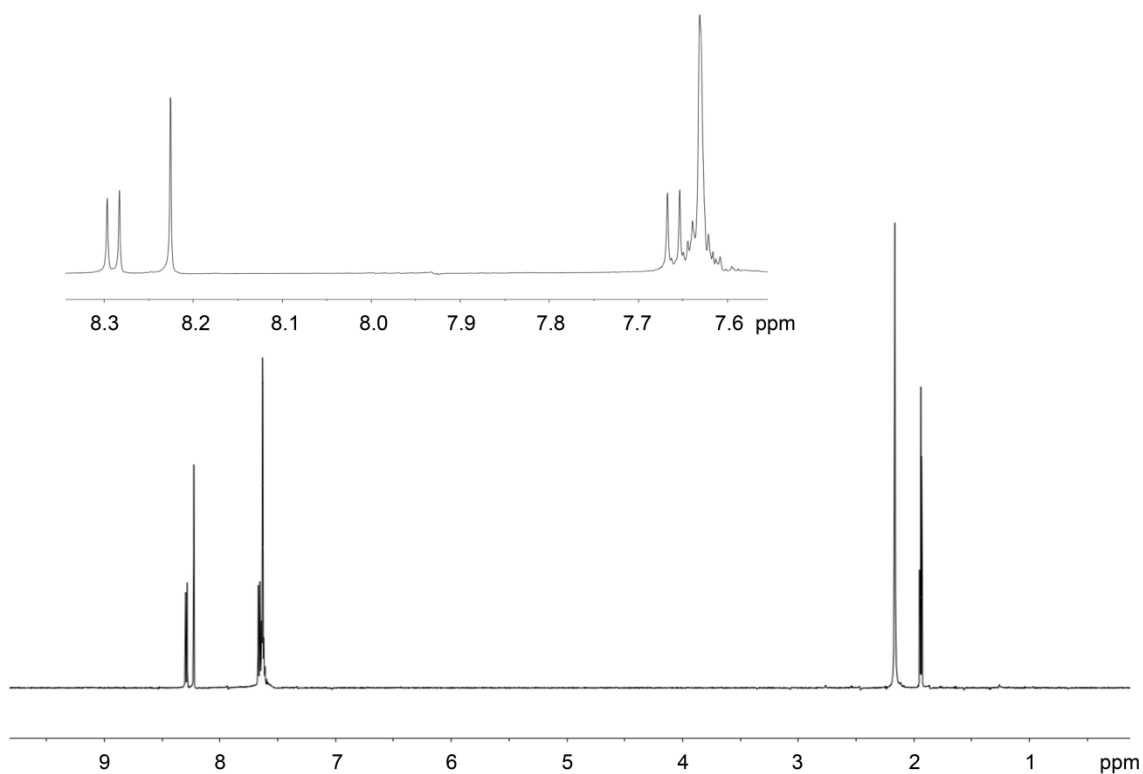


Figure S14: $^1\text{H-NMR}$ of **3** in CD_3CN .

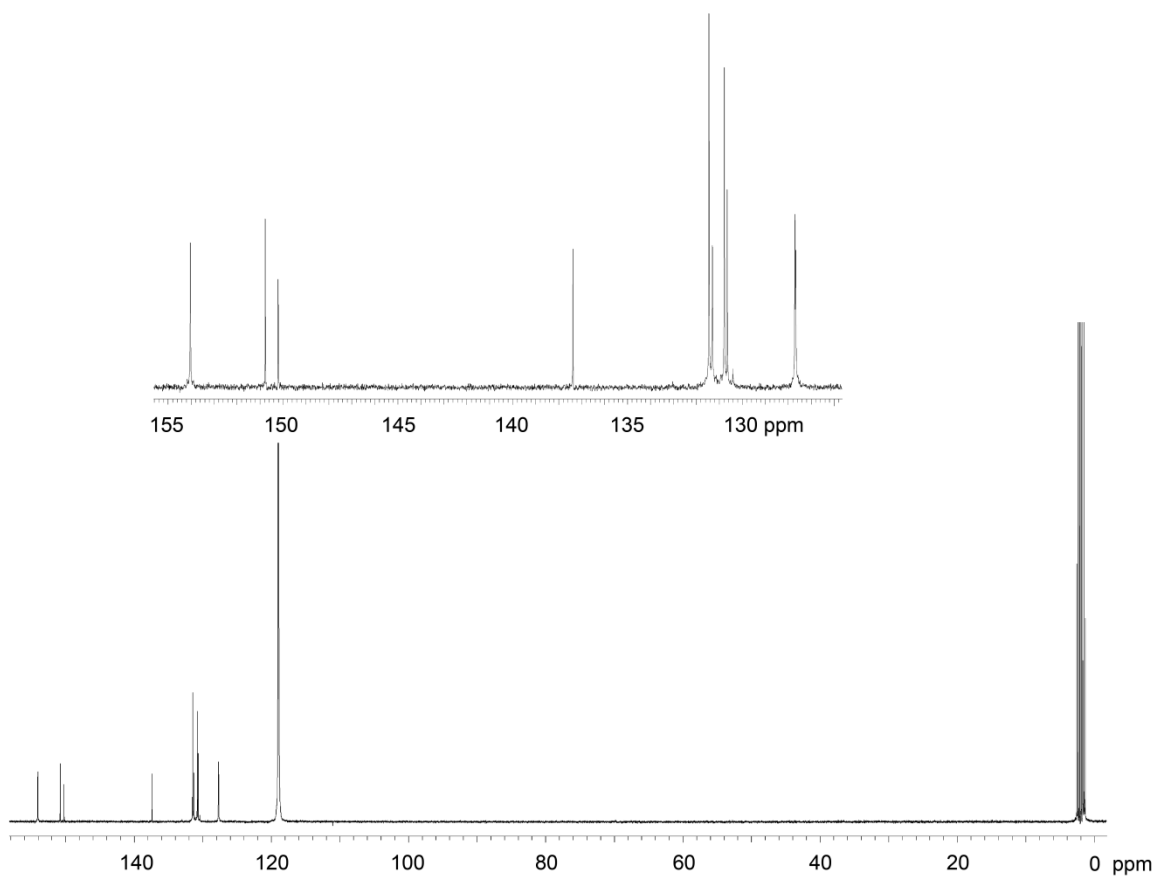


Figure S15: ^{13}C -NMR of **3** in CD_3CN . As expected from the symmetry of the complex, 10 unique carbons were observed.

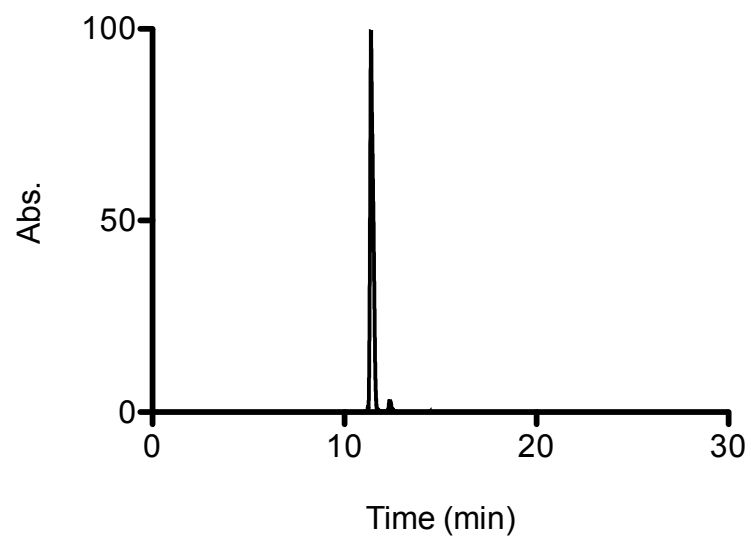


Figure S16: HPLC chromatograph to determine the purity of **3**. The purity of **3** was determined to be 98% by area using GraphPad Prism 5.0a.

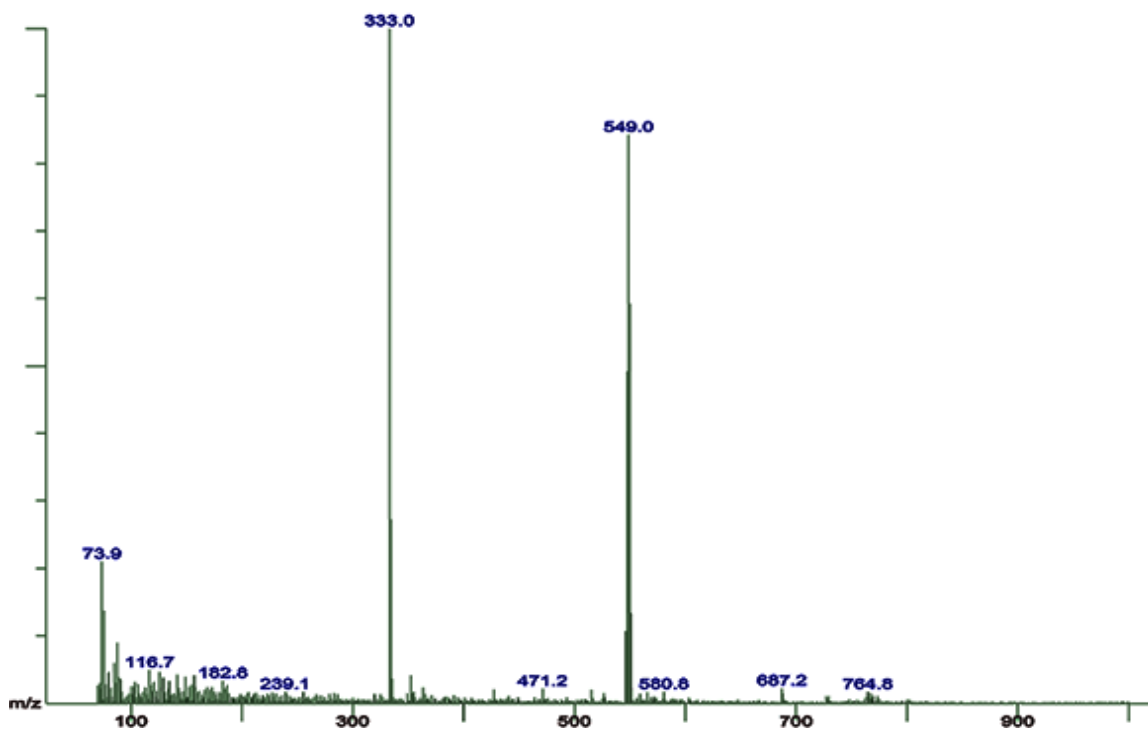


Figure S17: ESI-MS infusion of **3**. The ion at m/z 549.0 is the +2 form of the complex and the ion at m/z 333.0 is free dip. Free dip was not apparent in NMR analysis, which is indicative of complex degradation during ESI-MS infusion.

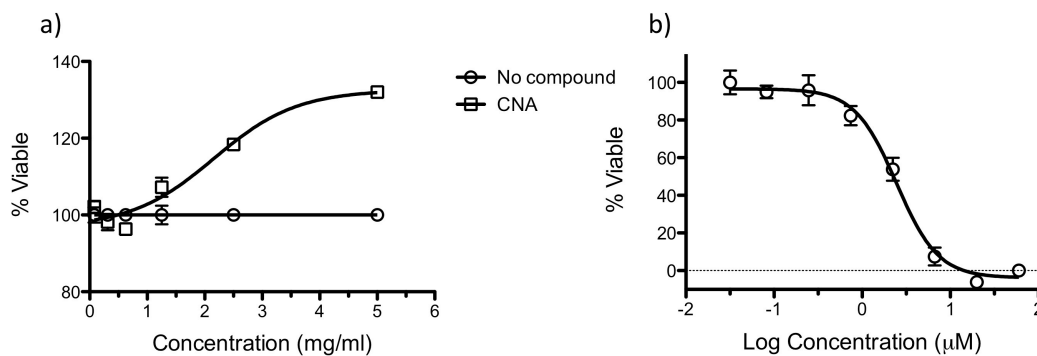


Figure S18. Analysis of cytotoxicity in A549 cells for a) CNAs and b) cisplatin. The CNAs induced a moderate increase in cell number, and the EC_{50} value for cisplatin routinely varies between 2-4 μM ($\text{EC}_{50} = 2.5 \mu\text{M}$ for data shown).

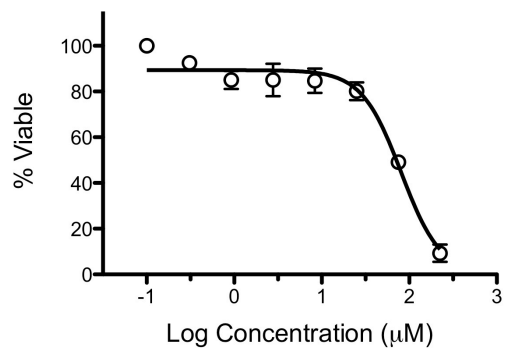


Figure S19. Analysis of cytotoxicity in A549 cells for dmbpy.

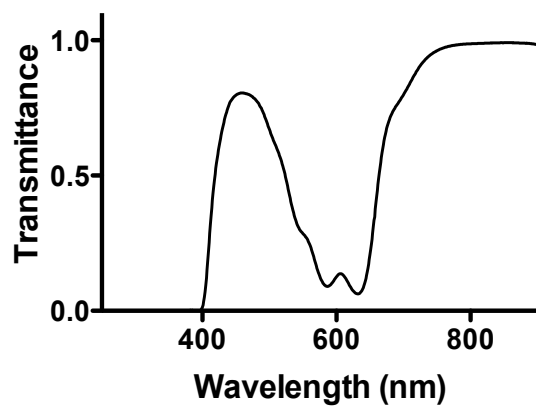


Figure S20. Transmittance spectrum of the NT43-941 optical filter.